Journal of Magnetism and Magnetic Materials 23 (1981) 333–341
North-Holland Publishing Company

SPECIFIC HEAT AND MAGNETIC SUSCEPTIBILITY OF MnF_2 AND $Mn_{0.98}Fe_{0.02}F_2$ NEAR T_N

P. NORDBLAD, L. LUNDGREN, E. FIGUEROA and O. BECKMAN
Department of Solid State Physics, Institute of Technology, University of Uppsala, Box 534, S-751 21 Uppsala, Sweden

Received 27 February 1981

The antiferro- to paramagnetic phase transition of the weakly anisotropic compound MnF_2 has been studied by means of heat capacity, magnetic susceptibility and thermal expansion measurements. The critical-point parameters associated with the specific heat indicate a transition according to the theoretical Ising-model. The temperature derivative of the parallel magnetic susceptibility times temperature ($d(\chi_\parallel T)/dT$) and the *c*-axis thermal expansion coefficient show a critical behaviour very similar to that of the specific heat. The influence of iron doping on the critical behaviour has been investigated by studies on $Mn_{0.98}Fe_{0.02}F_2$. Specific heat and magnetic susceptibility measurements show an unexpectedly sharp transition although some rounding off is noticed as compared to pure MnF_2.

1. Introduction

The anomalous behaviour of physical properties at phase transitions show striking similarities for such diverse media as fluids and magnetic materials. These observations are in accordance with the predictions from recent theories [1,2], which state that the critical behaviour is governed only by the space dimensionality n of the order parameter of the system (provided sufficiently short range interactions are dominating). From these theories critical-point parameters typical for different values of d and n can be calculated. In magnetic systems the dimensionality n is given by the number of degrees of freedom of the spin fluctuations. Three different models are applicable to magnetic systems:

- The Ising model ($n = 1$),
- The planar model ($n = 2$),
- The Heisenberg model ($n = 3$).

Each model gives a separate set of critical-point parameters. The magnetic specific heat C_m is characterized by the critical-point exponent α and the reduced temperature $t = |T - T_0|/T_0$ (T_0 is the transition temperature). Sufficiently close to the transition C_m can be expressed by the simple asymptotic equations:

$$C_m/R = A't^{-\alpha'} + B', \quad T < T_0, \tag{1'}$$

$$C_m/R = At^{-\alpha} + B, \quad T > T_0. \tag{1}$$

The scaling constraint implies $\alpha = \alpha'$ and the continuity constraint $B = B'$. For the space dimensionality $d = 3$ the Ising model predicts $\alpha = \alpha' \approx 0.1$ and $A/A' \approx 0.5$, the planar model $\alpha = \alpha' \approx 0$ and $A/A' \approx 1$, while the Heisenberg model gives $\alpha = \alpha' \approx -0.1$ and $A/A' \approx 1.5$ [3]. High accuracy specific heat measurements of two antiferromagnetic substances, the highly anisotropic compound FeF_2 [4] and the isotropic compound $RbMnF_3$ [5] have been performed far into the asymptotic region of the antiferro- to paramagnetic phase transition. The critical-point parameters obtained from these studies are in good agreement with those calculated from the theoretical Ising and Heisenberg models, respectively. In most experimental studies serious 'rounding effects' of the transition have been observed, however, which limit the possibility to determine accurate critical-point parameters from the asymptotic equations. In the analysis of these data first order correction terms have to be introduced in eq. (1) to extend the t-range for the scaling predictions [6]. In order to deduce accurate critical point parameters and possible cross-over

0304-8853/81/0000–0000/$02.50

effects of the spin dimensionality in the critical region improved experiments on antiferromagnetic materials in the asymptotic region near T_N are necessary.

Theoretical studies of critical behaviour have led to the prediction of several relations between different physical properties near phase transitions. For a simple antiferromagnet with predominantly short range interactions, Fisher [7] has postulated the following relation between the magnetic specific heat C_m and the parallel magnetic susceptibility $\chi_\parallel$:

$$C_m/R \approx K\partial(\chi_\parallel T)/\partial T, \quad (2)$$

where R is the gas constant and K is a slowly varying function of temperature. This relation should be valid even in the immediate critical region near the Néel temperature T_N. It should thus be possible to deduce the critical-point parameters associated with the magnetic specific heat of an antiferro- to paramagnetic phase transition from susceptibility measurements.

In this paper, the antiferro- to paramagnetic phase transition of MnF_2 and $Mn_{0.98}Fe_{0.02}F_2$ has been studied by means of specific heat and magnetic susceptibility measurements. MnF_2 has also been investigated by thermal expansion measurements.

Manganesedifluoride crystallizes in the body-centered tetragonal rutile structure with two formula units per unit cell. The pure compound is antiferromagnetically ordered below 67.3 K with the easy spin direction parallel to the tetragonal axis. The anisotropy energy is small (4.6×10^5 J/m^3 at 4.2 K [8]). The manganese atoms at the corners of the tetragonal unit cell form one sublattice and the central atoms a second sublattice.

From earlier measurements of the specific heat of MnF_2 [9,10] it has not been possible to deduce accurate critical-point parameters. Our previous measurements of the magnetic susceptibility of MnF_2 [11] compared with the experimental data on the magnetic specific heat obtained by Teaney [9] show that Fisher's relation, eq. (2), is in qualitative agreement with the experimental results.

The main purpose of this investigation of the antiferro- to paramagnetic phase transition of the weakly anisotropic compound MnF_2 is:

(i) Determine the critical-point parameters associated with the magnetic specific heat.
(ii) Characterize the nature (spin dimensionality) of the transition from the deduced critical-point parameters.
(iii) Check the validity of Fisher's relation in the immediate critical region on one and the same single crystal material.
(iv) Study the effect of iron doping on the critical behaviour of MnF_2 from measurements on $Mn_{0.98}Fe_{0.02}F_2$.
(v) Investigate the feasibility of a new technique for measurements of thermal expansion, particularly at magnetic phase transitions.

2. Experimental

2.1. Thermometry

Experiments on critical behaviour require high precision in the measurement of the sample temperature. Dauphinee and Preston-Thomas [12] have shown that fine commercial copper wire can be used as a precision thermometer in the temperature range 20–320 K, and they emphasize the possibility to attain excellent thermal contact between thermometer and sample with such a thermometer. In the present studies of specific heat, magnetic susceptibility and thermal expansion we have used copper wires (ϕ0.04 mm, length ≈1 m) as resistance thermometers. The resistance of the copper wire was measured with a four probe ac-method (300 Hz) with a relative resolution of ≈0.2 ppm, giving a temperature resolution better than 10 μK in the temperature range 55–80 K. The absolute accuracy of the thermometer is believed to be better than 0.1 K [12].

2.2. Specific heat

The standard heat-pulse technique was used in the heat capacity measurements. In the immediate vicinity of the transition heat pulses giving temperature increments (ΔT) as low as 1 mK were used in order to resolve the details of the specific heat peak. Away from the transition heat pulses giving temperature increments of around 10 mK were used. The heat pulses were all of 10 s duration. The sample to thermometer relaxation time was approximately 1 s. The temperature drifts, 60 s before and after the heat pulse, were recorded and the temperature change was

found from extrapolation to the center of the heat pulse. The temperature drifts were of the order of 5 μK per 10 s.

2.3. Magnetic susceptibility

A SQUID magnetometer [13] was used for the susceptibility measurements. The sample was glued to the sample holder (made of 5 N silver) by means of silver paint to provide good thermal contact. The thermometer (copper wire) and the heater (manganin wire) were bifilarly wound and glued to the sample holder. The sample was magnetized by a superconducting solenoid working in the persistent mode to achieve a highly stable magnetic field. The temperature of the sample was controlled by a proportional-integrating-differentiating (PID) regulator giving a temperature stability of ± 5 μK.

The susceptibility measurements were performed as follows: At a constant applied field (H) the change in magnetization (ΔM) for a temperature change (ΔT) is observed. Thereby the quantity $T\Delta M/H\Delta T$ is obtained. The absolute value of the magnetization (M) is found by observing the change of the magnetization from a reference temperature, where an M vs. H curve has been taken. If M is strictly proportional to H, we can derive the susceptibility χ and thus $\mathrm{d}(\chi T)/\mathrm{d}T$, which is the quantity of interest in this study. In the vicinity of the transition ($|T - T_N| < 30$ mK) ΔT's as small as 1.2 mK were used to avoid rounding effects of the peak of the measured curve. For such a small temperature change the relative change of the magnetization is 40–90 ppm, which is determined with a precision of about 1 ppm. It should be emphasized that the temperature derivative of the susceptibility is determined for each temperature increment ΔT directly from observed experimental quantities, and does not involve any numerical smoothing procedure.

2.4. Thermal expansion

A new method for thermal expansion measurements has been tested. Two counter connected coils are used to create an ac-field. The coils are designed to give a closely linear spatial dependence of the field along the symmetry axis of the two coils. A pick-up coil, attached to one end of the sample, is centered between the two coils. Length variations of the sample, which cause displacements of the pick-up coil, are detected by the corresponding change of the induced voltage in the pick-up coil. The arrangement allows a relative resolution of approximately 2×10^{-9} for a sample of 2 cm length ($\Delta l \approx 4 \times 10^{-11}$ m).

The measurements were performed as follows: The temperature of the sample is allowed to drift slowly and the changes in sample length are continuously recorded. In the immediate vicinity of the transition the temperature drift was $\approx$0.3 mK/min. The thermal expansion coefficient was found from numerical differentiation of the observed changes in length of the sample over temperature intervals of 1.5 mK close to T_N.

Details of the experimental techniques and apparatus for specific heat, magnetic susceptibility and thermal expansion measurements at magnetic phase transitions have been reported elsewhere [14].

3. Samples

3.1. MnF_2

An excellent quality single crystal block of pure MnF_2 was generously supplied to us by W.A. Hargreaves (OPTOVAC INC.). It had the dimensions $7 \times 9 \times 19$ mm^3 (mass 4.5777 g) with the longest side coinciding with the tetragonal axis of the crystal. The heat capacity as well as the thermal expansion measurements were performed on this single crystal. For the parallel magnetic susceptibility measurements a smaller piece ($1.5 \times 1.5 \times 4$ mm^3, mass 42.9 mg) was cut from this crystal using a low speed diamond wheel saw. The longest side of the crystal piece coincided with the c-axis of the crystal.

3.2. $Mn_{0.98}Fe_{0.02}F_2$

The $Mn_{0.98}Fe_{0.02}F_2$ single crystal was kindly provided to us by Prof. V. Jaccarino (University of California St. Barbara, USA). The shape of the crystal was a circular disc (Ø 10 mm, height 3 mm, mass 1.0330 g). The specific heat measurements were performed on this crystal. For the measurements of the parallel magnetic susceptibility a smaller piece ($1.4 \times 1.4 \times 3$ mm^3,

mass 24.5 mg) was cut from this crystal. The longest side of the crystal piece coincided with the tetragonal axis of the crystal.

4. Results

4.1. Specific heat of MnF_2

The measurements were performed in the temperature range $|T - T_N| < 10$ K where $T_N = 67.3$ K. The absolute values of the specific heat of MnF_2 from our measurements deviate by –0.1% at 60 K, –0.1% at 65 K, 26% at 67.3, –0.6% at 70 K and 0.1% at 75 K from the values obtained by Boo and Stout [10]. They performed measurements, between 10 and 300 K, on a large sample consisting of crystal pieces of MnF_2 (≈2 mm in size). Boo and Stout estimate their specific heat data to be accurate to 0.2% in the temperature range 40–200 K, except near T_N, where their data suffer from rounding effects. They suggest that the rounding near T_N might be due to a distribution of transition temperatures (of the order of 0.1 K) between the different crystal pieces in their sample.

Fig. 1 shows our specific heat data plotted together with the values obtained by Boo and Stout in a large temperature range; also plotted in the figure is the lattice contribution to the specific heat as calculated by

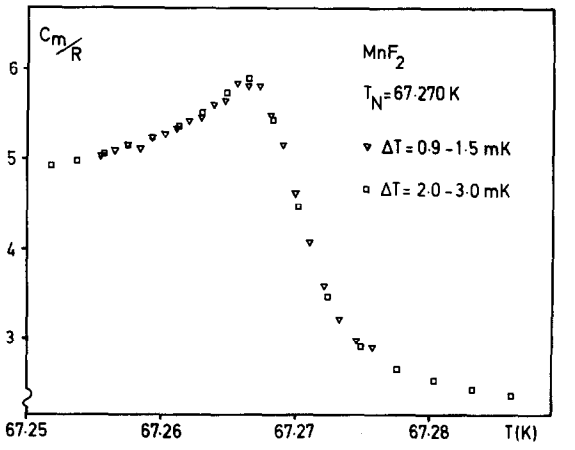

Fig. 2. Magnetic specific heat of MnF_2 close to T_N.

Boo and Stout. The magnetic part of the specific heat C_m was obtained by subtraction of the lattice contribution from the measured specific heat C_{tot}. Fig. 2 shows C_m/R in a linear temperature scale close to the transition. The transition temperature is by definition the point where C_m diverges or obtains a maximum value. In actual specific heat experiment the transition is rounded and the transition temperature is usually chosen to lie somewhere between the maximum and the inflection point of the C_m vs. T curve. In our experiment the distance between these two points is

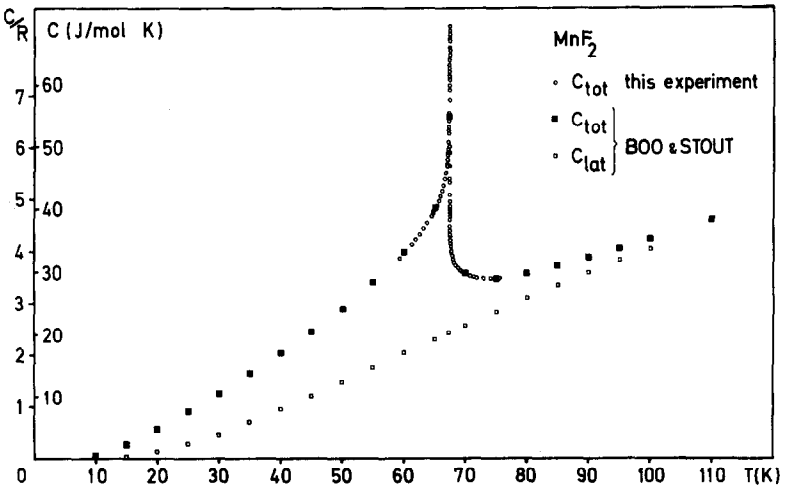

Fig. 1. Total specific heat (C_{tot}) of MnF_2 and the lattice contribution to the specific heat (C_{lat}) as calculated by Boo and Stout [10].

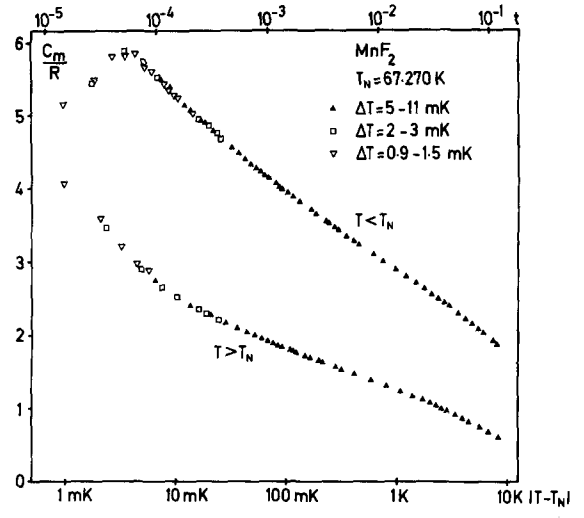

Fig. 3. Magnetic specific heat of MnF_2 plotted in a semilogarithmic diagram ($t = |T - T_N|/T_N$).

only about 3.5 mK or 5×10^{-5} in reduced temperature. In fig. 3 the magnetic specific heat is plotted in a semilogarithmic diagram as a function of $|T - T_N|$, with $T_N = 67.270$ K, i.e. the inflection point of the C_m vs. T curve.

To deduce the critical-point parameters with the constraints $\alpha = \alpha'$ and $B = B'$ the magnetic specific heat data were fitted to the asymptotic eqs. (1) and (1'), according to the following procedure: A preliminary value of T_N is chosen. C_m/R is plotted in a semilogarithmic diagram as a function of t (see fig. 3). The difference between C_m/R values corresponding to the same t value below T_N (C_m/R^-) and above T_N (C_m/R^+) is calculated for some t values. These differences are plotted in a logarithmic diagram as a function of t. From the slope of this curve a preliminary value of the critical-point exponent α is obtained. (With the constraints given above the logarithm of the difference between the eqs. (1') and (1) gives $\log(C_m/R^- - C_m/R^+) = -\alpha \log t + \log(A' - A)$.) The optimum fit to eqs. (1) and (1') is found by plotting C_m/R^+ and C_m/R^- as functions of $t^{-\alpha}$ for some choices of T_N and α close to the preliminary obtained values. The best possible fit gave: $T_N = 67.270$ K (the inflection-point of the C_m vs. T curve), $\alpha = \alpha' = 0.12$ and $A/A' = 0.50$. Temperature ranges of fit: $T < T_N$: $7 \times 10^{-5} < t < 4 \times 10^{-3}$, $T > T_N$: $2 \times 10^{-4} < t < 5 \times 10^{-3}$.

4.2. Parallel magnetic susceptibility of MnF_2

The susceptibility measurements were performed as described above, in the temperature range $|T - T_N| < 10$ K. The absolute value of the magnetization was determined at the maximum point of the $\chi_\parallel$ vs. T curve. The susceptibility value 1.321×10^{-2} (SI) from our previous measurements on a spherical MnF_2 single crystal [11] was used as an absolute calibration value of the susceptibility. The measurements were performed in an applied field of 0.03 T (300 G). In the temperature region $|T - T_N| < 20$ mK an applied field of 0.01 T was also used, but no significant changes of the features of the peak in the $d(\chi_\parallel T)/dT$ vs. T curve could be observed. In fig. 4, $Kd(\chi_\parallel T)/dT$ ($K = 77$, eq. (2)) is plotted together with the magnetic specific heat in a semilogarithmic diagram as a function of $|T - T_N|$. T_N has been chosen at the inflection point of the $d(\chi_\parallel T)/dT$ vs. T curve.

In table 1 numerical values of $\chi_\parallel T$, $d(\chi_\parallel T)/dT$, U_m/R and C_m/R from 0–100 K have been summarized. The susceptibility data originate from the present measurements, the C_m/R data are taken from Boo and Stout [10]. The magnetic energy U_m/R data have been determined from numerical integration of experimental C_m/R values, which have been normalized at 100 K according to Boo and Stout [10] using the theoretical model by Rushbrooke and Wood [15]. An independent, crude check of U_m/R is obtained from a

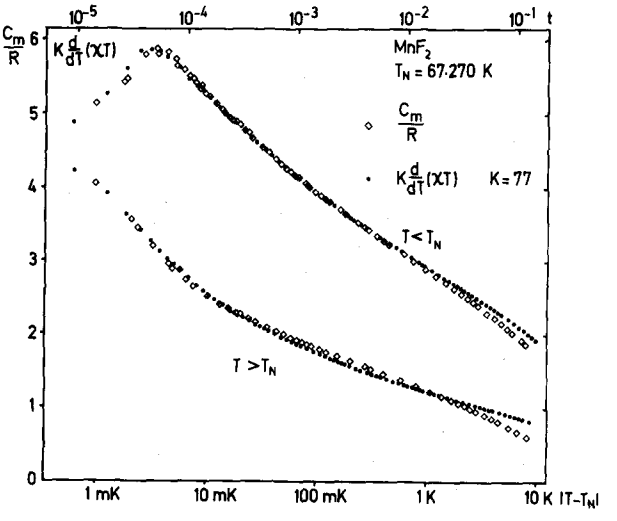

Fig. 4. C_m/R and $Kd(\chi_\parallel T)/dT$ of MnF_2 plotted in a semilogarithmic diagram ($t = |T - T_N|/T_N$).

Table 1
Magnetic energy of MnF_2

T (K)	$\chi_\parallel T$ (K)	$\partial(\chi_\parallel T)/\partial T$ ($\times 10^2$)	$-U_m/R$ (K)	C_m/R
0	0		95.07	0
10			94.93	0.057
15			94.29	0.222
20			92.70	0.423
25	0.0643	0.763	90.12	0.614
30	0.1081	0.989	86.59	0.805
35	0.1633	1.229	82.25	0.936
40	0.2304	1.477	77.19	1.087
45	0.3112	1.740	71.39	1.243
50	00.4052	2.025	64.72	1.419
55	0.5133	2.340	57.12	1.636
60	0.6409	2.720	48.25	1.943
65	0.7911	3.387	37.26	2.531
67.3	0.8798		30.48	
70	0.9246	1.363	26.97	0.996
75	0.9843	1.107	23.03	0.624
80	1.036	0.971	20.37	0.463
85	1.082	0.875	18.28	0.357
90	1.123	0.799	16.77	0.292
95	1.162	0.739	15.46	0.231
100	1.198	0.688	14.40	0.186

direct calculation of the exchange energy $U_{exch} = -NJq\boldsymbol{S}_i \cdot \boldsymbol{S}_j$, where q is the number of nearest neighbours. With $J_2 = -1.76$ K, $q = 8$ and $J_1 = 0.3$ K, $q = 2$ [17] we obtain $U_m/R = -92$.

4.3. Thermal expansion of MnF_2

The thermal expansion along the tetragonal axis of the single crystal block was measured in the temperature range $|T - T_N| < 10$ K. In fig. 5 $\alpha_c = (1/l)(dl/dT)$ is plotted as a function of $|T - T_N|$ in a semilogarithmic diagram, using the inflection point of the α_c vs. T curve as T_N. The linear thermal expansion coefficient shows the same general features as the specific heat.

4.4. Specific heat and parallel magnetic susceptibility of $Mn_{0.98}Fe_{0.02}F_2$

The measurements were performed in the temperature range $|T - T_N| < 10$ K with T_N equal to 68.13 K. The magnetic part of the specific heat was found from subtraction of the lattice contribution from the measured specific heat. The lattice contribution to the

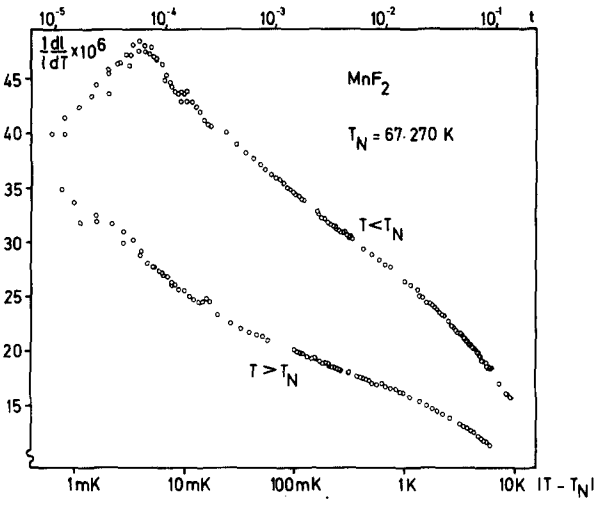

Fig. 5. The thermal expansion coefficient of the c-axis of MnF_2 as a function of $\log|T - T_N|$ ($t = |T - T_N|/T_N$).

specific heat of $Mn_{0.98}Fe_{0.02}F_2$ was calculated as a mixture of 98% MnF_2 and 2% FeF_2, using the values of the lattice contribution given by Boo and Stout for MnF_2 [10] and Stout and Catalano for FeF_2 [16]. The peak of the C_m vs. T curve is somewhat more rounded than the peak of the same curve for MnF_2; the distance between the maximum point and the inflection point is about 6 mK for $Mn_{0.98}Fe_{0.02}F_2$.

The susceptibility measurements were made in a

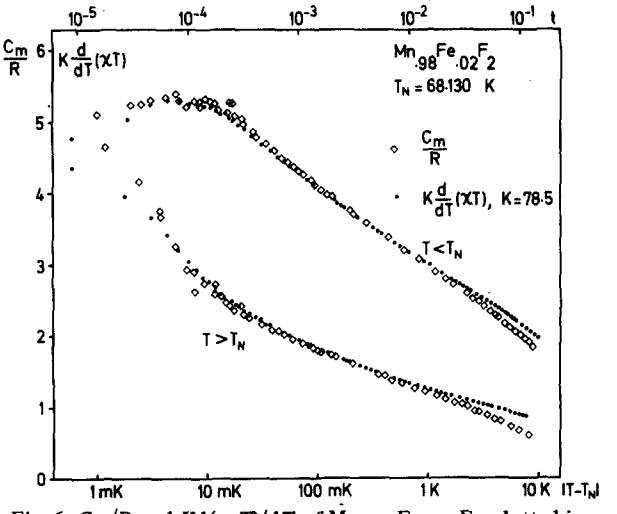

Fig. 6. C_m/R and $Kd(\chi_\parallel T)/dT$ of $Mn_{0.98}Fe_{0.02}F_2$ plotted in a semilogarithmic diagram ($t = |T - T_N|/T_N$).

similar way as for MnF_2. The absolute susceptibility value at the maximum of the $\chi_\parallel$ vs. T curve was attributed the same value 1.321×10^{-2} (SI) for calibration as for the pure MnF_2 sample. In fig. 6 C_m/R and $Kd(\chi_\parallel T)/dT$ ($K = 78.5$, eq. (2)) are shown in the same semilogarithmic diagram, using $T_N = 68.13$ K i.e. the inflection points of the C_m and $d(\chi_\parallel T)/dT$ vs. T plots.

5. Discussion

Manganesedifluoride is only weakly anisotropic and might therefore be considered as an example of a Heisenberg model antiferromagnet. However, the critical-point parameters deduced from our specific heat measurements ($\alpha = \alpha' \approx 0.12$ and $A/A' \approx 0.50$) are in accordance with the theoretical Ising model values. Neutron diffraction studies [17] of the spin fluctuations show that the longitudinal correlation length diverges, whereas the transverse correlation length is finite due to suppression by the anisotropy field. The longitudinal spin fluctuations for $T > T_N$ show critical parameters $\gamma \approx 1.24$, $\nu \approx 0.63$ and $\eta \approx 0.05$ in close agreement with the theoretical Ising model parameters for a bcc lattice ($\gamma \approx 1.25$, $\nu \approx 0.643$ and $\eta \approx 0.056$) [18]. In addition, our previous susceptibility measurements [11] indicate Ising-like behaviour since the perpendicular susceptibility shows a much less pronounced divergence than the parallel susceptibility at T_N ($|T - T_N| < 0.2$ K)

$$d(\chi_\perp T)/dT = 0.07\, d(\chi_\parallel T)/dT + 1.33 \times 10^{-2}. \qquad (3)$$

For $|T - T_N| \geq 0.3$ K, both above and below T_N, there is a pronounced change of curvature of the C_m vs. $\log |T - T_N|$ curve (see fig. 3), which can be interpreted as a change from spin dimensionality $n = 1$ at T_N to spin dimensionality $n = 3$ away from T_N. Fisher and Aharony [19] have shown that for isotropic dipolar ferromagnets a crossover from Heisenberg to dipolar dominated character should be expected when approaching the transition. Aharony [20] estimates the exponent characteristic for the dipolar interactions to be $\alpha \approx -0.03$. In contrast to the ferromagnetic case, theoretical calculations on antiferromagnets [20] indicate that the critical parameters should maintain their short range interaction values at the transition. From these arguments it is difficult to understand the Ising nature of the transition in MnF_2 and a possible cross-over to Heisenberg behaviour away from the transition. The weakly anisotropic antiferromagnets with dipolar interactions $MnCl_2 \cdot 4H_2O$ [21], $MnBr_2 \cdot 4H_2O$ [6], $GdAlO_3$ [22] and $GdVO_4$ [23] also display Ising-like behaviour at the transition, but for these antiferromagnets no cross-over effects have been observed in the critical region.

A characteristic feature of the specific heat results on the above mentioned dipolar antiferromagnets [24] is an anomalous increase of the specific heat in the vicinity of T_N for $T > T_N$. This sudden rise is also found for MnF_2, but the onset of the anomaly is strongly dependent on the quality of the sample. In our previous susceptibility measurements on MnF_2 [11], which were made on a lower quality crystal than the one used in the present study, the sudden rise occurs for $t \leq 5 \times 10^{-4}$ while the deviation from a pure exponential form was found at $t \leq 2 \times 10^{-4}$ in the present specific heat measurements. A shift towards higher t values of the anomaly is also evident for the iron doped MnF_2 crystal (see fig. 6). In contrast to these observations, the measurements on the highly anisotropic antiferromagnet FeF_2 [4] and on the isotropic antiferromagnet $RbMnF_3$ [5] do not display this anomalous behaviour.

Fig. 4 shows C_m/R and $Kd(\chi_\parallel T)/dT$ ($K = 77$) plotted together in a semilogarithmic diagram. As can be seen even the details of the specific heat peak are reproduced by the susceptibility behaviour, which verifies the general predictions by Fisher (eq. (2)). However, small but significant deviations from strict proportionality between C_m and the susceptibility behaviour can be observed for $T > T_N$.

Thermal expansion and specific heat measurements [5] on the cubic antiferromagnet $RbMnF_3$ have proved the validity of the exact thermodynamic relation:

$$C_p = T(\partial S/\partial T)_t + VT(\partial P/\partial T)_t \alpha_p.$$

Since the partial derivatives have weak temperature dependence, the specific heat and the linear thermal expansion coefficient ($\frac{1}{3}\alpha_p$) should have the same asymptotic behaviour. In MnF_2 we find that the linear thermal expansion coefficient of the c-axis is in close linear relation to the specific heat in the vicinity of T_N.

The specific heat peak of the iron doped crystal,

$Mn_{0.98}Fe_{0.02}F_2$, is more rounded than the peak of the pure crystal, but considering the high "impurity" content the transition is surprisingly sharp. The curvature of the C_m vs. $\log|T - T_N|$ curve indicates an Ising nature of the transition. The change of curvature occurs for a t value which is significantly higher than that of the crossover for the pure MnF_2 crystal. In the pure FeF_2 compound [4] there is no sign of a deviation from an Ising-like behaviour in the critical region ($t \leqslant 10^{-1}$).

The peak of the $d(\chi_\parallel T)/dT$ curve for $Mn_{0.98}Fe_{0.02}F_2$ shows a similar rounding as the specific heat curve. Fig. 6 shows C_m/R and $Kd(\chi_\parallel T)/dT$ ($K = 78.5$) plotted in a semilogarithmic diagram. Obviously Fisher's relation [2] is valid also for the 'imperfect' system $Mn_{0.98}Fe_{0.02}F_2$. The theoretical models on critical behaviour generally prescribe a pure exponential form infinitely close to the transition. However, the experimental results always show rounding effects and thereby deviations from a pure exponential behaviour. These rounding effects are commonly attributed to imperfections in the samples investigated. In MnF_2, we find that Fisher's relation is valid even at temperatures close to the transition where imperfection effects give marked deviations from the ideal exponential behaviour. This observation implies an extended validity of Fisher's relation and thereby a wider universiality than the common theoretical models whose applicability on real materials is limited.

The transition temperature of $Mn_{0.98}Fe_{0.02}F_2$ is 0.86 K higher than the transition temperature of the pure compound. This increase is about four times larger than would be expected from a linear extrapolation with iron content from T_N of MnF_2 (67.3 K) to T_N of FeF_2 (78.4 K).

In the derivation of the Fisher relation (eq. (2)) [7] Fisher finds the following relation between the magnetic energy and the parallel magnetic susceptibility:

$$U_m/R = K[(\chi_\parallel T)_\infty - \chi_\parallel T]. \quad (4)$$

The asymptotic value $(\chi_\parallel T)_\infty$ is equivalent to the Curie constant, which for MnF_2 has the numerical value 2.32 K. Neglecting any temperature dependence of K the Fisher relation (eq. (2)) is obtained by differentiating eq. (4). In fig. 7 we have plotted K as found from eqs. (2) and (4). The numerical values of $\chi_\parallel T$ and U_m/R are listed in table 1. In spite of some uncertainties in the calculation of U_m/R the very large discrepancy between the calculated K-values is remarkable. This is quite surprising with respect to the excellent validity of Fisher's relation in its final form (eq. (2)).

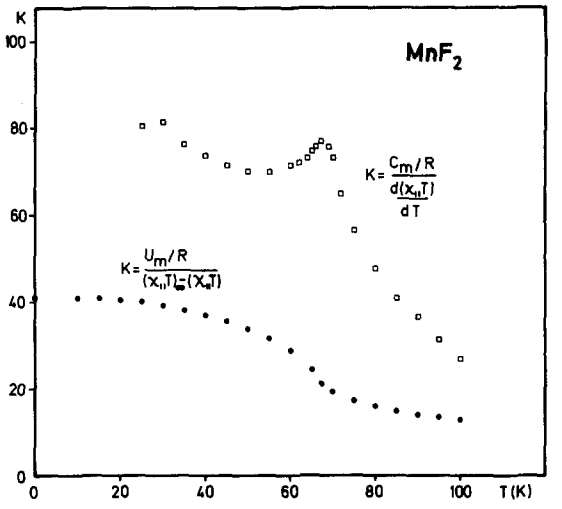

Fig. 7. The proportionality function K found from eq. (2) and eq. (4).

Acknowledgements

We are grateful to doc. Sven Hörnfeldt, who suggested the new method for the thermal expansion measurements. Financial support from the Swedish Natural Science Research Council (NFR) is gratefully acknowledged. One of us (E.F.) would like to express his gratitude to the Swedish Institute and SIDA for a research fellowship.

References

[1] K.G. Wilson and J. Kogut, Phys. Rev. C12 (1974) 75.
[2] M.E. Fisher, Rev. Mod. Phys. 46 (1974) 597.
[3] M. Barmatz, P.C. Hohenberg and A. Kornblit, Phys. Rev. B12 (1975) 1947.
[4] M. Chirwa, L. Lundgren, P. Nordblad and O. Beckman, J. Magn. Magn. Mat. 15–18 (1980) 457.
[5] A. Kornblit and G. Ahlers, Phys. Rev. B8 (1973) 5163.
[6] J.E. Rives and D.P. Landau, Phys. Rev. B17 (1978) 4426.

[7] M.E. Fisher, Phil. Mag. 7 (1962) 1731.
[8] U. Gäfvert, L. Lundgren, P. Nordblad, B. Westerstrandh and O. Beckman, Solid State Commun. 23 (1977) 9.
[9] D.T. Teaney, Phys. Rev. Lett. 14 (1965) 898.
[10] W.O.J. Boo and J.W. Stout, J. Chem. Phys. 65 (1976) 3929.
[11] P. Nordblad, L. Lundgren, E. Figueroa, U. Gäfvert and O. Beckman, Phys. Scripta 20 (1979) 105.
[12] T.M. Dauphinee and H. Preston-Thomas, Rev. Sci. Instr. 25 (1954) 885.
[13] K. Gramm, L. Lundgren and O. Beckman, Phys. Scripta 13 (1976) 93.
[14] L. Lundgren and P. Nordblad, UPTEC 80 25 R (1980).
[15] J.S. Rushbrooke and P.J. Wood, Mol. Phys. 1 (1958) 257.
[16] J.W. Stout and E. Catalano, J. Chem. Phys. 23 (1955) 2013.
[17] M.B. Schulhof, P. Heller, R. Nathans and A. Linz, Phys. Rev. B1 (1970) 2304.
[18] M.E. Fisher and R. Burford, Phys. Rev. 156 (1967) 583.
[19] A. Aharony and M.E. Fisher, Phys. Rev. B8 (1973) 3323.
[20] A. Aharony, Phys. Rev. B8 (1973) 3349.
[21] G.S. Dixon and J.E. Rives, Phys. Rev. 177 (1969) 871.
[22] J.D. Cashion, A.H. Cooke, T.L. Thorp and M.R. Wells, Proc. Roy. Soc. A318 (1970) 473.
[23] J.D. Cashion, A.H. Cooke, L.A. Hoel, D.M. Marnin and M.R. Wells, Proc. Colloq. Intern. de CNRS No. 180 (1970) 417.
[24] C. Domb and J.A. Wyles, J. Phys. C2 (1969) 2435.